IR + Raman - IR- and Raman-Spectroscopy

Protocol for the PC 2 lab course by

Vincent Kümmerle & Elvis Gnaglo & Julian Brügger

University of Stuttgart

authors:	Vincent Kümmerle, 3712667 st187541@stud.uni-stuttgart.de
	Elvis Gnaglo, 3710504 st189318@stud.uni-stuttgart.de
	Julian Brügger, 3715444 st190050@stud.uni-stuttgart.de
group number:	A05
date of experiment:	21.01.2026
supervisor:	Mansha Shafquath
submission date:	January 23, 2026

Abstract:

Contents

1 Theory

[1]

2 Procedure

To simulate and calculate the vibrational normal modes, the program `Avogadro2` was used. The structures of the molecules methane, chloromethane, dichloromethane, dibromomethane, chloroform, deuterated chloroform, tetrachloromethane and tetrachloroethylene were built, their geometry was optimized and the optimized coordinates were used to calculate the vibrational modes with the `ORCA` software, resulting in a list of IR and Raman frequencies and intensities for each molecule.
In the experimental part, the Raman spectra of dichloromethane, dibromomethane, chloroform, deuterated chloroform, tetrachloromethane and tetrachloroethylene were measured and analysized with the `WPenlighten` software. The IR spectra of dichloromethane, dibromomethane, chloroform and tetrachloroethylene were measured using an ATR spectrometer and analysized with the `Opus` software.

3 Results and Analysis

3.1 Methane

3.1.1 IR

The calculated vibrational modes of methane are summarized in Table 1 with the corresponding wavenumber, intensitiy and vibration type of each mode.

Tab. 1: Listed are the calculated wavenumbers and intensities of the IR signals of CH_4 with the corresponding type of the vibrational mode.

signal	wavenumber $\tilde{\nu}$ / cm^{-1}	intensity / $KM{\cdot}mol^{-1}$	vibration type
1	1313.45	13.30	asym. bending
2	1313.68	13.25	asym. bending
3	1313.73	13.25	asym. bending
4	1530.79	0	sym. bending
5	1531.05	0	sym. bending
6	3019.38	0	sym. stretching
7	3152.03	17.69	asym. stretching
8	3152.33	17.64	asym. stretching
9	3152.45	17.64	asym. stretching

As can be seen in Table 1, only the asymmetric bending and stretching modes are IR-active, while the symmetric bending and stretching modes are IR-inactive. Furthermore, the asymmetric stretching mode shows the highest wavenumber among the IR-active modes, meaning it requires the most energy to be excited.

3.1.2 Raman

The calculated Raman-active vibrational modes of methane are summarized in Table 2 with the corresponding wavenumber, Raman intensity and vibration type of each mode.

Tab. 2: Listed are the calculated wavenumbers and intensities of the Raman signals of CH_4 with the corresponding type of the vibrational mode.

signal	wavenumber $\tilde{\nu}$ / cm^{-1}	Raman intensity / $Å^4 \cdot amu^{-1}$	vibration type
1	1313.38	1.64419	asym. bending
2	1313.61	1.6422	asym. bending
3	1314.1	1.6484	asym. bending
4	1531.00	27.4565	sym. bending
5	1531.09	27.449	sym. bending
6	3019.41	145.177	sym. stretching
7	3150.24	62.8181	asym. stretching
8	3150.27	62.8724	asym. stretching
9	3150.79	62.8305	asym. stretching

In contrast to the IR spectrum, both the symmetric bending and stretching modes are Raman-active. The symmetric stretching mode shows the highest Raman intensity among all vibrational modes, indicating that it is most prominent mode to be observed in a Raman spectrum.

3.2 Chloromethane

3.2.1 IR

3.2.2 Raman

3.3 Dichloromethane

3.3.1 IR

The measured IR spectrum of dichloromethane is shown in Figure 1, plotting the intensity of the absorption against the wavenumber $\tilde{\nu}$.

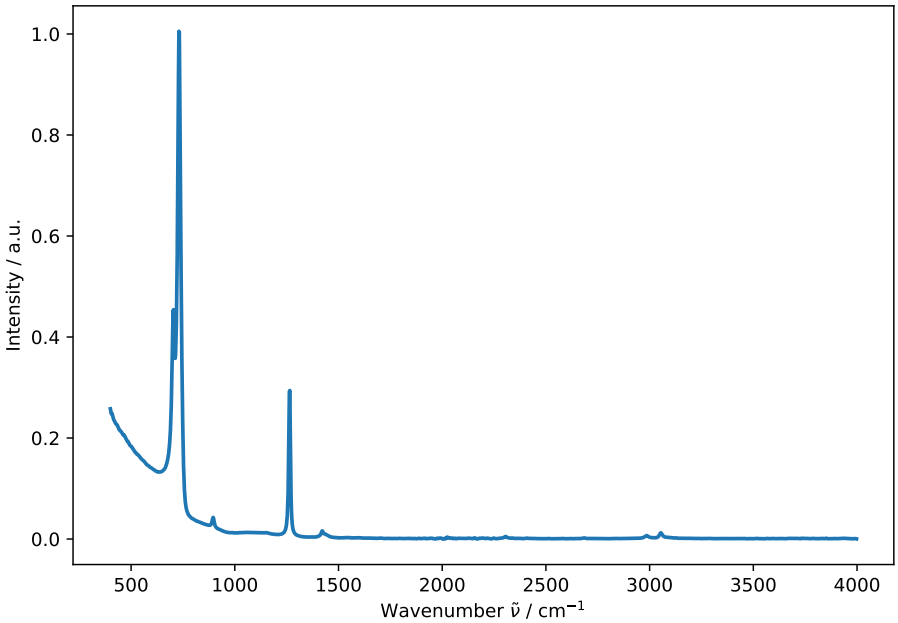

Fig. 1: Measured IR spectrum of dichloromethane.

Tab. 3: Listed are the measured wavenumbers and intensities of the IR signals of CH_2Cl_2.

signal	wavenumber $\tilde{\nu}$ / cm^{-1}	intensity / a.u.
1	704.00	0.45
2	730.53	1.01
3	895.82	0.04
4	1265.17	0.29
5	1422.29	0.02

Tab. 4: Listed are the simulated wavenumbers and intensities of the vibrational modes of CH_2Cl_2.

Mode	Wavenumber $\tilde{\nu}$ / cm^{-1}	Intensity / $KM \cdot mol^{-1}$
1	277.23	0.64
2	703.86	14.19
3	733.80	137.83
4	889.17	1.20
5	1153.54	0.00
6	1272.86	41.21
7	1441.46	0.01
8	3107.43	9.81
9	3194.30	0.64

3.3.2 Raman

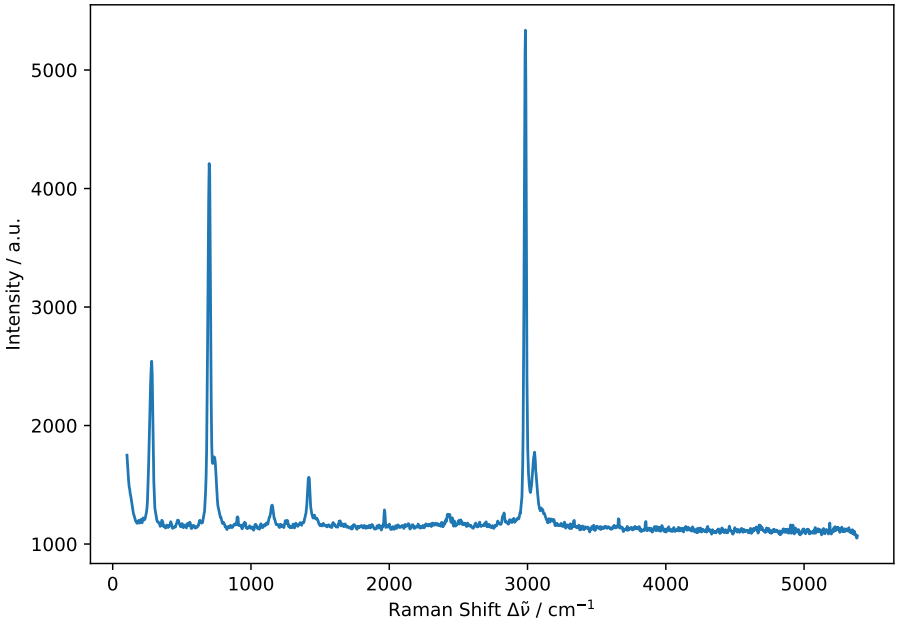

Fig. 2: Measured raman spectrum of dichloromethane.

Tab. 5: Listed are the measured Raman shifts and intensities of the signals of CH_2Cl_2.

signal	Raman Shift $\Delta\tilde{\nu}$ / cm^{-1}	intensity / a.u.
1	281.99	2542.67
2	697.77	4210.67
3	1418.07	1563.33
4	2984.85	5336.00
5	3051.13	1775.33

Tab. 6: Listed are the simulated wavenumbers and raman intensities of the vibrational modes of CH_2Cl_2.

Mode	Wavenumber $\tilde{\nu}$ / cm^{-1}	Raman Intensity / $Å^4$ amu^{-1}
1	277.06	6.83
2	703.48	12.27
3	732.67	5.02
4	888.90	3.13
5	1153.83	11.78
6	1272.67	3.01
7	1441.64	12.42
8	3106.65	108.70
9	3193.09	62.65

3.4 Dibromomethane

3.4.1 IR

The measured IR spectrum of dibromomethane is shown in Figure 3, plotting the intensity of the absorption against the wavenumber $\tilde{\nu}$.

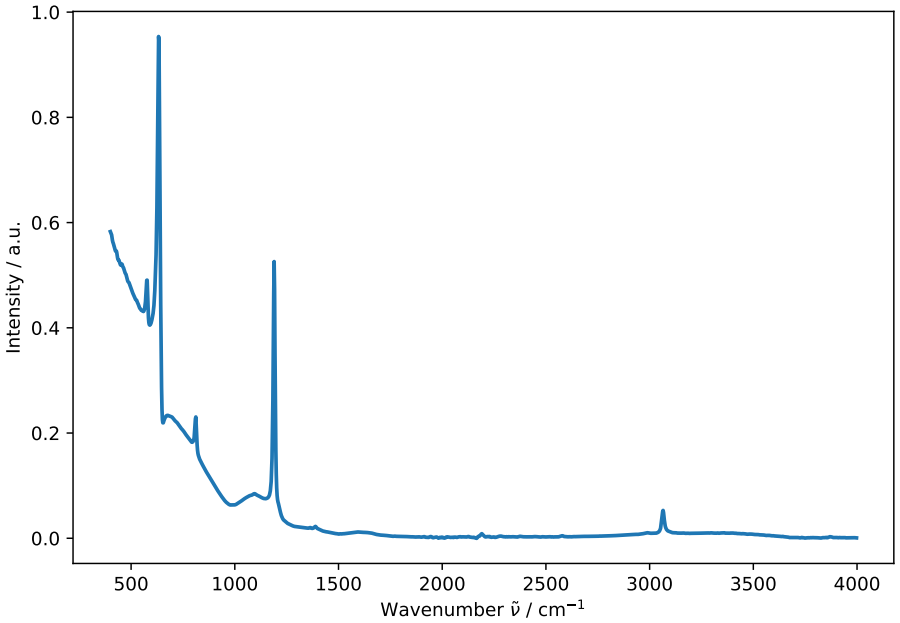

Fig. 3: Measured IR spectrum of dibromomethane.

Tab. 7: Listed are the measured wavenumbers and intensities of the IR signals of CH_2Br_2.

signal	wavenumber $\tilde{\nu}$ / cm^{-1}	intensity / a.u.
1	455.05	0.52
2	577.49	0.49
3	632.58	0.95
4	677.48	0.23
5	812.16	0.23
6	1095.80	0.08
7	1189.66	0.53
8	1389.64	0.02
11	3064.97	0.05

Tab. 8: Listed are the simulated wavenumbers and intensities of the vibrational modes of CH_2Br_2.

Mode	Wavenumber $\tilde{\nu}$ / cm^{-1}	Intensity / $KM \cdot mol^{-1}$
1	168.72	0.08
2	573.58	4.08
3	628.31	98.95
4	806.07	4.64
5	1101.92	0.00
6	1205.80	65.32
7	1412.95	0.00
8	3126.16	1.92
9	3221.84	1.28

3.4.2 Raman

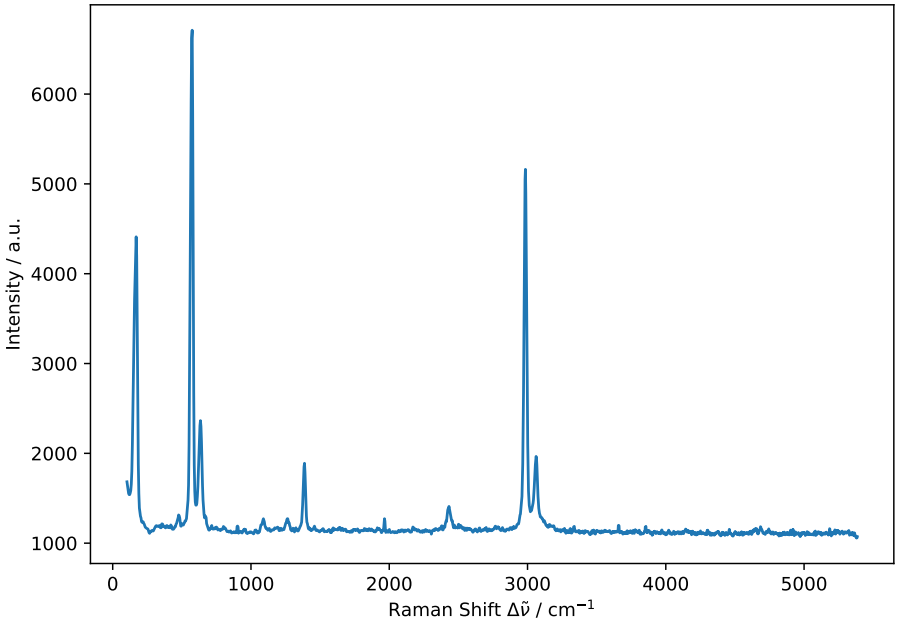

Fig. 4: Measured raman spectrum of dibromomethane.

Tab. 9: Listed are the measured Raman shifts and intensities of the signals of CH_2Br_2.

signal	Raman Shift $\Delta\tilde{\nu}$ / cm^{-1}	intensity / a.u.
1	169.61	4410.67
2	574.79	6711.00
3	634.60	2364.33
4	1387.16	1889.33
5	2432.07	1409.00
6	2984.85	5162.00
7	3062.11	1965.67

Tab. 10: Listed are the simulated wavenumbers and raman intensities of the vibrational modes of CH_2Br_2.

Mode	Wavenumber $\tilde{\nu}$ / cm^{-1}	Raman Intensity / $Å^4$ amu^{-1}
1	168.56	5.37
2	574.64	13.43
3	629.71	5.36
4	806.60	2.41
5	1102.17	8.43
6	1205.71	0.74
7	1413.22	13.77
8	3125.63	97.24
9	3221.31	58.05

3.5 Chloroform

3.5.1 IR

The measured IR spectrum of chloroform is shown in Figure 5, plotting the intensity of the absorption against the wavenumber $\tilde{\nu}$.

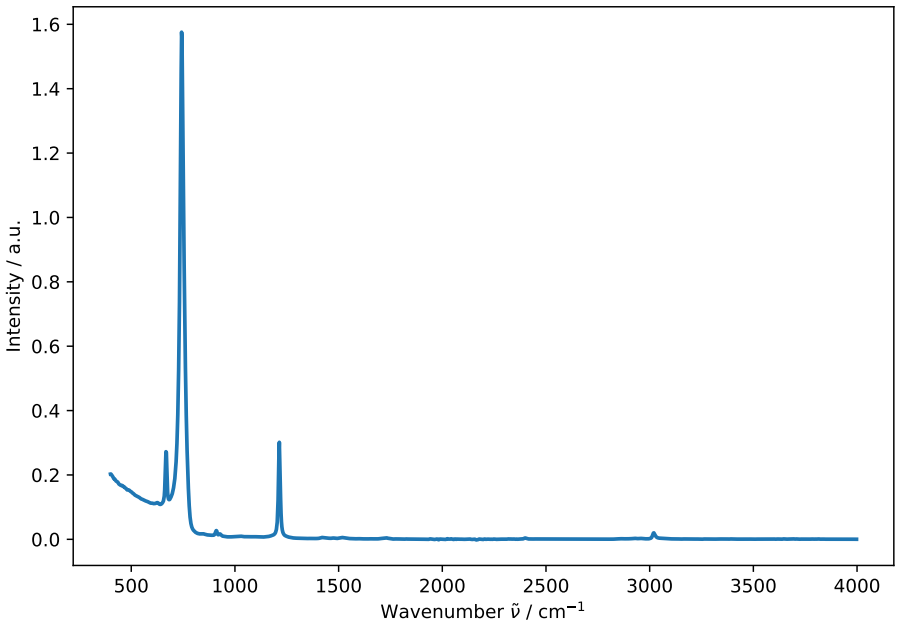

Fig. 5: Measured IR spectrum of chloroform.

Tab. 11: Listed are the measured wavenumbers and intensities of the IR signals of $CHCl_3$.

signal	wavenumber $\tilde{\nu}$ / cm^{-1}	intensity / a.u.
1	626.46	0.11
2	667.27	0.27
3	742.78	1.58
4	910.10	0.03
5	928.47	0.02
6	1214.15	0.30
7	3020.07	0.02

Tab. 12: Listed are the simulated wavenumbers and intensities of the vibrational modes of $CHCl_3$.

Mode	Wavenumber $\tilde{\nu}$ / cm^{-1}	Intensity / $KM \cdot mol^{-1}$
1	254.78	0.06
2	254.97	0.06
3	362.33	0.46
4	665.85	7.26
5	741.92	167.74
6	742.13	167.67
7	1220.08	22.80
8	1220.17	22.76
9	3169.43	0.22

3.5.2 Raman

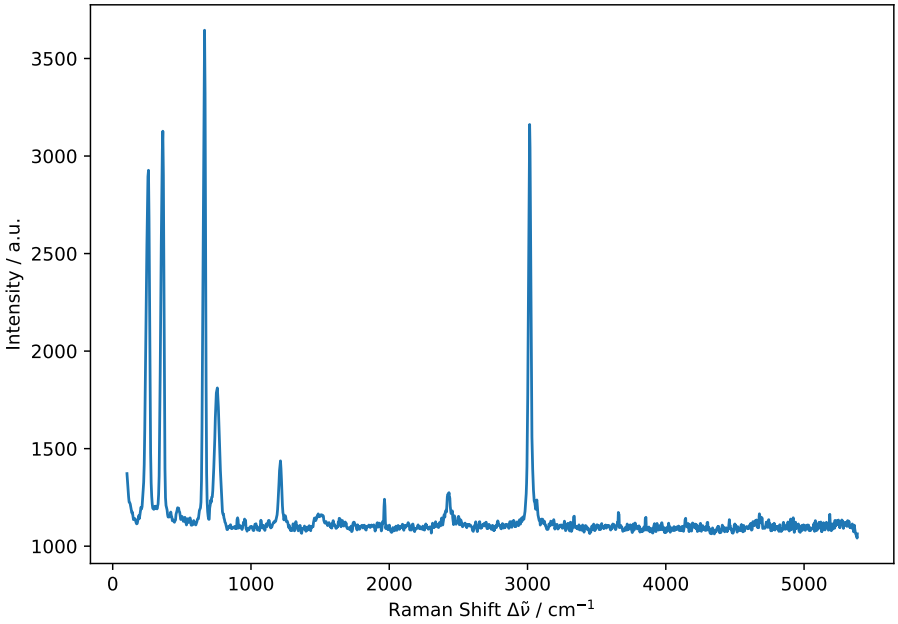

Fig. 6: Measured raman spectrum of chloroform.

Tab. 13: Listed are the measured Raman shifts and intensities of the signals of $CHCl_3$.

signal	Raman Shift $\Delta\tilde{\nu}$ / cm^{-1}	intensity / a.u.
1	258.84	2927.00
2	362.65	3127.33
3	664.38	3645.00
4	756.86	1811.33
5	1213.44	1437.33
6	3015.32	3161.67

Tab. 14: Listed are the simulated wavenumbers and raman intensities of the vibrational modes of $CHCl_3$.

Mode	Wavenumber $\tilde{\nu}$ / cm^{-1}	Raman Intensity / $Å^4$ amu^{-1}
1	254.60	5.14
2	255.07	5.13
3	362.22	8.69
4	665.69	9.80
5	740.88	3.08
6	741.45	3.07
7	1220.22	6.04
8	1220.68	6.05
9	3168.77	77.28

3.6 Deuterated Chloroform

3.6.1 IR

Tab. 15: Listed are the simulated wavenumbers and intensities of the vibrational modes of $CDCl_3$.

Mode	Wavenumber $\tilde{\nu}$ / cm^{-1}	Intensity / KM·mol^{-1}
1	253.69	0.06
2	253.88	0.06
3	360.12	0.50
4	646.14	6.66
5	717.83	125.46
6	717.98	125.28
7	909.65	63.16
8	909.66	63.19
9	2342.61	0.74

3.6.2 Raman

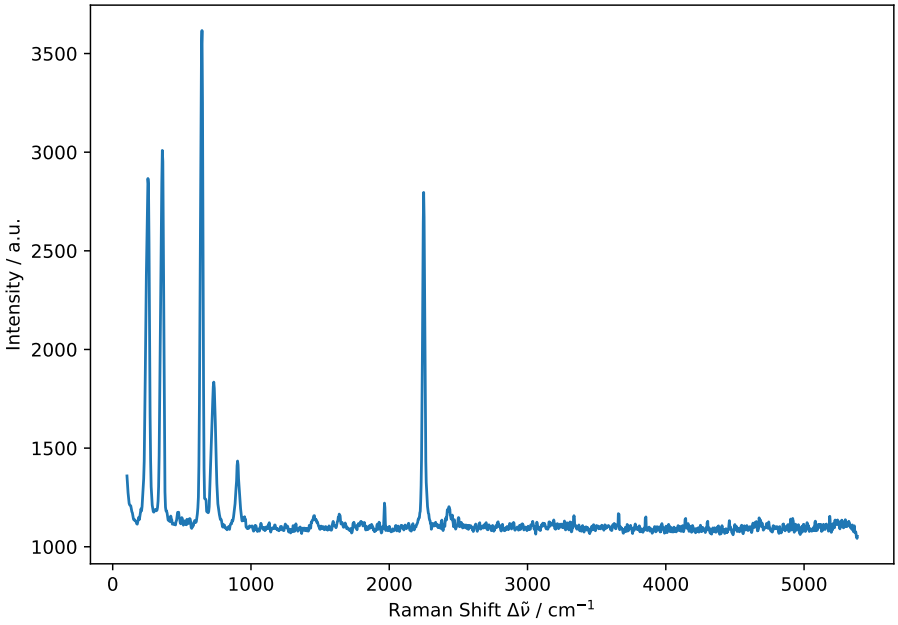

Fig. 7: Measured raman spectrum of deuterated chloroform.

Tab. 16: Listed are the measured Raman shifts and intensities of the signals of $CDCl_3$.

signal	Raman Shift $\Delta\tilde{\nu}$ / cm^{-1}	intensity / a.u.
1	254.97	2866.67
2	358.83	3009.00
3	645.78	3616.67
4	731.05	1834.67
5	903.05	1434.67
6	2248.93	2796.00

Tab. 17: Listed are the simulated wavenumbers and raman intensities of the vibrational modes of $CDCl_3$.

Mode	Wavenumber $\tilde{\nu}$ / cm^{-1}	Raman Intensity / $Å^4$ amu^{-1}
1	254.60	5.14
2	255.07	5.13
3	362.22	8.69
4	665.69	9.80
5	740.88	3.08
6	741.45	3.07
7	1220.22	6.04
8	1220.68	6.05
9	3168.77	77.28

3.7 Tetrachloromethane

3.7.1 IR

Tab. 18: Listed are the simulated wavenumbers and intensities of the vibrational modes of CCl_4.

Mode	Wavenumber $\tilde{\nu}$ / cm^{-1}	Intensity / KM·mol^{-1}
1	212.71	0.00
2	212.89	0.00
3	310.72	0.06
4	310.82	0.06
5	310.88	0.06
6	451.20	0.00
7	754.80	185.52
8	755.02	185.61
9	755.51	185.58

3.7.2 Raman

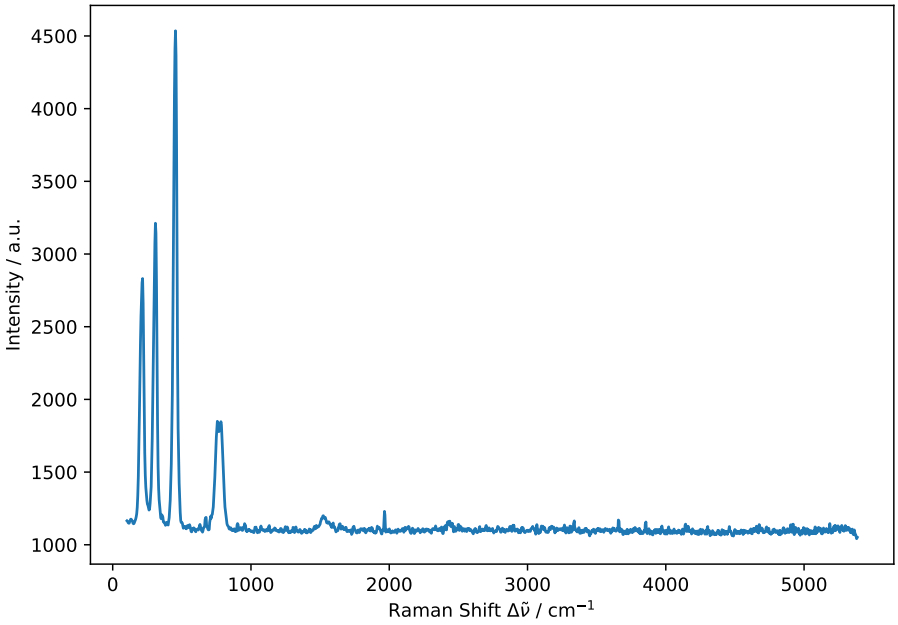

Fig. 8: Measured raman spectrum of tetrachloromethane.

Tab. 19: Listed are the measured Raman shifts and intensities of the signals of CCl_4.

signal	Raman Shift $\Delta\tilde{\nu}$ / cm^{-1}	intensity / a.u.
1	216.25	2831.33
2	308.95	3211.67
3	454.10	4535.33
4	756.86	1849.33

Tab. 20: Listed are the simulated wavenumbers and Raman intensities of the vibrational modes of CCl_4.

Mode	Wavenumber $\tilde{\nu}$ / cm^{-1}	Raman Intensity / $Å^4$ amu^{-1}
1	212.71	4.18
2	212.91	4.17
3	310.52	5.39
4	310.84	5.40
5	311.16	5.40
6	451.08	16.40
7	753.44	1.55
8	754.26	1.56
9	754.60	1.54

3.8 Tetrachloroethylene

3.8.1 IR

The measured IR spectrum of tetrachloroethylene is shown in Figure 9, plotting the intensity of the absorption against the wavenumber $\tilde{\nu}$.

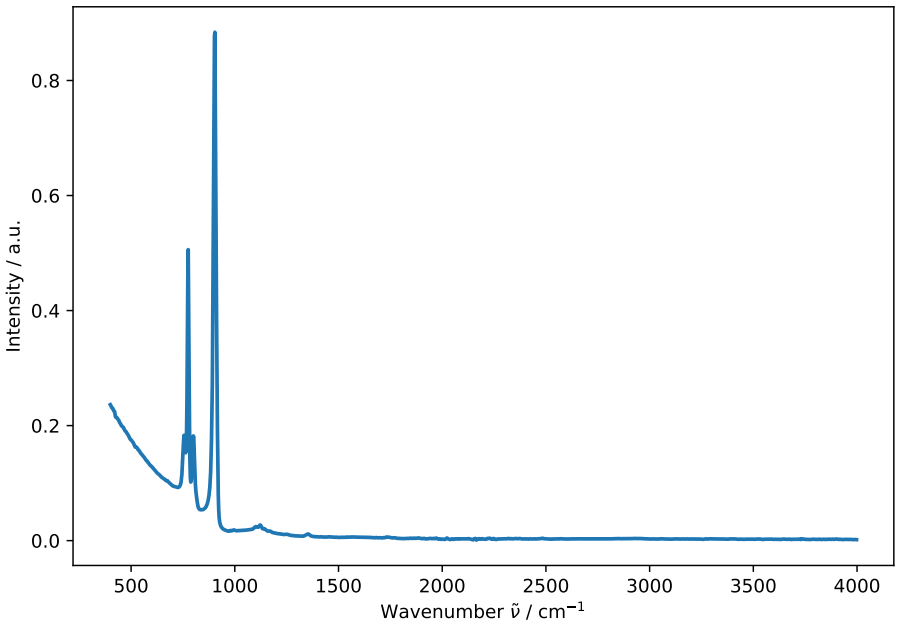

Fig. 9: Measured IR spectrum of tetrachloroethylene.

By visual inspection of the IR spectrum in Figure 9, six absorption signals can be identified, which are listed with their corresponding wavenumbers and intensities in Table 21.

Tab. 21: Listed are the measured wavenumbers and intensities of the IR signals of C_2Cl_4 with the corresponding type of the vibrational mode.

signal	wavenumber $\tilde{\nu}$ / cm^{-1}	intensity / a.u.	vibration type
1	755.02	0.18	
2	775.42	0.51	asym. stretching
3	799.91	0.18	
4	903.98	0.88	asym. stretching
5	1122.32	0.03	
6	1354.95	0.01	

The calculated vibrational modes of tetrachloroethylene are summarized in Table 22 with the corresponding wavenumber, intensitiy and vibration type of each mode.

Tab. 22: Listed are the simulated wavenumbers and intensities of the vibrational modes of C_2Cl_4.

Mode	Wavenumber $\tilde{\nu}$ / cm^{-1}	Intensity / $KM \cdot mol^{-1}$
1	97.18	0.00
2	174.89	0.96
3	234.77	0.00
4	286.90	0.51
5	310.42	0.03
6	342.99	0.00
7	447.02	0.00
8	514.19	0.00
9	774.46	82.16
10	895.52	202.05
11	978.50	0.00

As can be seen in Table 22, the most intense IR-active modes are found at wavenumbers of 774.46 cm^{-1} and 895.52 cm^{-1}, which correspond well to the measured signals at 755.02 cm^{-1} and 903.98 cm^{-1} in Figure 9.

In comparison to the simulated IR spectrum of chloroform with the wavenumbers and vibrational modes in Table 11, tetrachloroethylene shows additional IR-active modes in the low wavenumber region below 500 cm^{-1}, which can be attributed to the increased number of atoms in the molecule leading to more vibrational modes. Furthermore, tetrachloroethylene

3.8.2 Raman

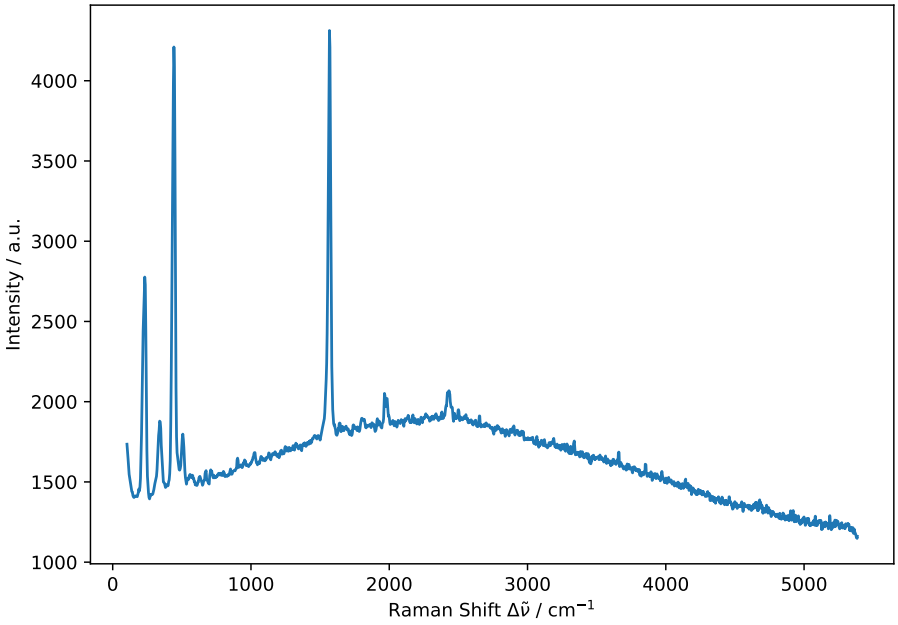

Fig. 10: Measured raman spectrum of tetrachloroethylene.

Tab. 23: Listed are the measured Raman shifts and intensities of the signals of C_2Cl_4.

signal	Raman Shift $\Delta\tilde{\nu}$ / cm^{-1}	intensity / a.u.
1	231.76	2776.67
2	339.67	1879.00
3	442.71	4210.33
4	1567.61	4313.00
5	2432.07	2068.33

Tab. 24: Listed are the simulated wavenumbers and Raman intensities of the vibrational modes of C_2Cl_4.

Mode	Wavenumber $\tilde{\nu}$ / cm^{-1}	Raman Intensity / $Å^4$ amu^{-1}
1	97.98	0.00
2	174.79	0.00
3	234.62	5.56
4	289.22	0.00
5	310.02	0.00
6	342.83	4.61
7	446.81	15.61
8	517.38	3.22
9	774.24	0.00
10	895.62	0.00
11	978.54	0.44
12	1623.90	48.63

In comparison to the calculated IR-active modes in Table 22, the Raman-active modes in Table 24 show a different pattern, with the most intense Raman-active mode found at a wavenumber of 1623.90 cm^{-1}, which does not correspond to any of the most intense IR-active modes.

4 Discussion

5 Conclusion

6 References

[1] H. Dilger, *2025-pc2-script-en*, **2025**.